6. The expression "surfactant-silicate" is used here as a comprehensive term for materials synthesized using a mixture of surfactant and silica species, regardless of the particular structure.
7. The transformation between the lamellar and hexagonal mesophases was observed after freeze-drying, as well as air-drying, the filtered samples.
8. Addition of trimethylbenzene (TMB) to the reaction mixture stabilizes the lamellar mesophase. Experiments have shown that the 31(±1) Å repeat distance for the layered material shown in Figs. 2A and 3 is preserved over a range of TMB concentrations between 0.5 and 3.0 M, whereas at lower TMB concentrations the hexagonal mesostructure is the favored product. Stabilization of the lamellar mesophase likely occurs because TMB dissolved within the surfactant hydrocarbon assemblies contributes to the hydrophobic chain volume. This increase in surfactant chain volume increases the value of A_0 at which the lamellar-to-hexagonal mesophase transformation occurs, according to a simple geometric model (*13*). Thus, the mesostructural transformation depicted in Fig. 2 is a consequence of hydrothermal removal of TMB from within the surfactant chain assembly, combined with an increase in A_0. This conclusion is supported by separate experiments which show that addition of TMB to the aqueous phase inhibits the transformation from a lamellar to a hexagonal mesostructure.
9. R. K. Harris, C. T. G. Knight, W. E. Hull, *ACS Symp. Ser.* 194, 79 (1982); C. T. G. Knight, R. G. Kirkpatrick, E. Oldfield, *J. Magn. Reson.* 78, (1988); A. V. McCormick and A. T. Bell, *Catal. Rev. Sci. Eng.* 31, 97 (1989).
10. R. K. Iler, *The Chemistry of Silica* (Wiley, New York, 1979), p. 182.
11. C. J. Brinker, G. W. Scherer, *Sol-Gel Science* (Academic Press, New York, 1990), p. 100.
12. K. Hagakawa and J. C. T. Kwac, *Surfactant Sci. Ser.* 37, 189 (1991).
13. J. Charvolin and J. F. Sadoc, *J. Phys.* 48, 1559 (1987). J. N. Israelachvili [in *Surfactants in Solution*, K. L. Mittal and P. Bothorel, Eds. (Plenum, New York, 1987), vol. 4, p. 3] proposed the dimensionless parameter $g = V/A_0\ell_c$ as a means of determining the preferred configuration of a surfactant assembly, where V is the volume of the hydrophobic chain and ℓ_c is the characteristic chain length. According to this treatment, spherical micelles will form if $g < 1/3$, cylindrical micelles if $1/3 < g < 1/2$, vesicles or bilayers if $1/2 < g < 1$, and inverted micelles if $g > 1$.
14. As discussed in (*7*), the presence of TMB in the reaction mixture can, but does not always, require a swelling response in surfactant systems.
15. A. Weiss, *Clays and Clay Minerals. Proceedings of the National Conference on Clays and Clay Minerals* (Earl Ingerso, New York, 1961), vol. 10, p. 191.
16. A. Weiss, *Angew. Chem. Int. Ed. Engl.* 20, 850 (1981).
17. The hexagonal shape of the mesopores can be determined from the y intercept of a plot of d spacings versus the number of carbon atoms for different chain length surfactants, corrected for the head-group diameter.
18. Calculated from d spacings, volumetric considerations (based on a measured void fraction of 0.65), and x-ray diffraction refinements based on the use of cylinder- and hexagonal-prismatic-rod-packing as models.
19. A. Monnier and G. D. Stucky, unpublished work.
20. T. Yanagisawa, T. Shimizu, K. Kuroda, C. Kato, *Bull. Chem. Soc. Jpn.* 63, 988 (1990).
21. P. Mariani, V. Luzzati, H. Delacroix, *J. Mol. Biol.* 204, 165 (1988).
22. A periodic minimal surface is the smallest surface separating a volume into two equal parts, given a certain periodic constraint.

23. We thank J. Israelachvili, J. Zasadzinski (UCSB), C. Kresge, D. Olson, J. Beck, J. Vartuli, and J. Higgins (Mobil) for helpful discussions. This research was funded by Air Products, du Pont, the MRL Program of the National Science Foundation under award DMR 9123048, the Office of Naval Research (G.D.S.), the NSF Science and Technology Center for Quantized Electronic Structures (grant DMR91-20007), the NSF/NYI program, and the Camille and Henry Dreyfus Foundation (B.F.C.) and through fellowships by the FNRS (A.M.) and the DFG (F.S.).

26 April 1993; accepted 8 July 1993

An Unnatural Biopolymer

Charles Y. Cho, Edmund J. Moran,* Sara R. Cherry, James C. Stephans, Stephen P. A. Fodor, Cynthia L. Adams, Arathi Sundaram, Jeffrey W. Jacobs, Peter G. Schultz†

A highly efficient method has been developed for the solid-phase synthesis of an "unnatural biopolymer" consisting of chiral aminocarbonate monomers linked via a carbamate backbone. Oligocarbamates were synthesized from *N*-protected *p*-nitrophenyl carbonate monomers, substituted with a variety of side chains, with greater than 99 percent overall coupling efficiencies per step. A spatially defined library of oligocarbamates was generated by using photochemical methods and screened for binding affinity to a monoclonal antibody. A number of high-affinity ligands were then synthesized and analyzed in solution with respect to their inhibition concentration values, water/octanol partitioning coefficients, and proteolytic stability. These and other unnatural polymers may provide new frameworks for drug development and for testing theories of protein and peptide folding and structure.

Polypeptides have been the focus of considerable attention with respect to their structure and folding, biological function, and therapeutic potential. The development of efficient solid-phase methodology for the synthesis of peptides (*1*), peptide derivatives (*2*), and large peptide libraries (*3–8*) has greatly facilitated these studies. The development of efficient methods for the synthesis of unnatural biopolymers (*9–11*) composed of building blocks other than amino acids may provide new frameworks for generating macromolecules with novel properties. For example, polymers with improved pharmacokinetic properties (such as membrane permeability and biological stability) might facilitate drug discovery, and polymers with altered conformational or hydrogen-bonding properties may provide increased insight into biomolecular structure and folding. We report the highly efficient solid-phase synthesis of oligocarbamate polymers from a pool of chiral aminocarbonates and the synthesis and screening of a library of oligocarbamates for their ability to bind a monoclonal antibody (mAb).

The oligocarbamate backbone (Fig. 1), in contrast to that of peptides, consists of a chiral ethylene backbone linked through relatively rigid carbamate groups. The α carbon, like that of peptides, is substituted with side chains that contain a variety of functional groups. Although the β carbon is unsubstituted in our initial target, additional backbone modifications (and conformational restriction) can be incorporated via alkylation of the β carbon or the carbamyl nitrogen. Oligocarbamates were synthesized from a pool of optically active *N*-protected aminocarbonates (Fig. 2) which, in turn, were derived from the corresponding optically active amino alcohols. The latter are either commercially available or can be prepared in chiral form by reduction of the *N*-hydroxysuccinimidyl or pentafluorophenyl esters of *N*-protected amino acids (*12*). The α-amino group was protected with the use of either nitroveratryl chloroformate (*13*) (NVOC-Cl) (for photochemical deprotection) or fluorenylmethyl-*N*-hydroxysuccinimidyl carbonate (Fmoc-OSu) (for base-catalyzed deprotection) (*14*). When necessary, side chains were protected as acid-labile *tert*-butyl esters, ethers, or carbamates. Protected amino alcohols were converted to the corresponding *N*-protected *p*-nitrophenyl carbonate monomers by reaction with *p*-nitrophenyl chloroformate in pyridine/CH_2Cl_2, generally in >80% yield. The carbonate monomers are stable for months at room temperature.

Solid-phase synthesis of oligocarbamates involves the sequential base-catalyzed or light-dependent deprotection of the α-amino group of the growing polymer chain followed by coupling to the next protected *p*-nitrophenyl carbonate monomer (Fig. 2). The *N*-protected "hydroxy-terminal" residue was covalently attached to polystyrene resin containing either *N*-protected *p*-alkoxybenzyl amino

C. Y. Cho, E. J. Moran, S. R. Cherry, J. C. Stephans, P. G. Schultz, Department of Chemistry, University of California, Berkeley, Berkeley, CA 94720.
S. P. A. Fodor, C. L. Adams, A. Sundaram, J. W. Jacobs, Affymax Research Institute, 4001 Miranda Avenue, Palo Alto, CA 94304.

*Present address: Ontogen Corporation, 2325 Camino Vida Roble, Carlsbad, CA 92009.
†To whom correspondence should be addressed.

acid ester (*15*) or 4-(2′-4′-dimethoxyphenyl-aminomethyl)-phenol (*16*) linkers. A typical coupling cycle involved: (i) deprotection of the resin Fmoc group by treatment with 20% piperidine in *N*-methylpyrrolidinone (NMP); (ii) washing of deprotected resin with NMP; (iii) coupling with 100 mM Fmoc carbonate monomer in 50 mM diisopropylethylamine (DIEA), 200 mM hydroxybenzotriazole (HOBt) in NMP for 4 hours at 25°C; and (iv) washing of resin with NMP. Side chain deprotection and cleavage from the resin were carried out as described for peptide synthesis (*17*). The products and yields of individual coupling reactions were monitored by analytical reversed-phase high-performance liquid chromatography (HPLC) and quantitative ninhydrin tests (*18*). Overall coupling yields were greater than 99% per step. Oligocarbamates were purified by preparative HPLC and characterized by fast atom bombardment mass spectrometry and nuclear magnetic resonance spectroscopy (*19*).

In order to demonstrate that libraries of oligocarbamates can be generated and screened for receptor binding, an oligocarbamate library was synthesized by using a light-directed parallel synthesis method previously described for the generation of oligopeptide libraries (*4*). This approach permits the spatially addressable synthesis and screening of individual oligocarbamates for receptor binding, thereby obviating the need for sequence analysis. Synthesis was carried out with NVOC-protected monomers that were deprotected by irradiation at 365 nm (*4*). A library containing 256 oligocarbamates was synthesized with a binary masking strategy with the parent sequence AcI^{c}F^{c}A^{c}S^{c}K^{c}I^{c}F^{c}L^c (this library contains all possible deletions of the parent sequence) (*4*, *20*). Carbamate coupling yields on the glass surface were determined as previously described for peptide couplings and were of comparable efficiency (≥90%) (*4*).

The oligocarbamate library was then screened for its ability to bind the α-AcY^{c}K^{c}F^{c}L^c mAb, 20D6.3 (*21*), which was prepared by standard methods from BALB/C mice immunized with the keyhole limpet hemocyanin conjugate of AcY^{c}K^{c}F^{c}L^{c}G-OH (*22*) (G-OH represents a terminal Gly residue) (*21*, *23*). The aminopropyl-derivatized glass surface containing the oligocarbamate library was treated with 20D6.3 in 50 mM tris, 150 mM NaCl buffer, pH 7.4, containing 10% calf serum at room temperature. Antibody-oligocarbamate complexes were then detected by scanning epifluorescent microscopy with a goat α-mouse fluorescein-conjugated secondary antibody (Fig. 3) (*4*). The oligocarbamates AcK^{c}F^{c}L^{c}G-OH, AcF^{c}K^{c}F^{c}L^{c}G-OH, AcY^{c}K^{c}F^{c}L^{c}G-OH, AcA^{c}K^{c}F^{c}L^{c}G-OH, and AcI^{c}F^{c}L^{c}G-OH, which were among the 10 highest affinity ligands based on fluorescence intensities, were then synthesized on an Applied Biosystems model 431A peptide synthesizer. Competition enzyme-linked immunosorbent assay experiments with AcY^{c}K^{c}F^{c}L^{c}G–bovine serum albumin conjugates revealed that all of these ligands bound to 20D6.3 in solution with IC_{50} values between 60 and 180 nM (*22*). In contrast, specific binding of the ligand AcY^{c}I^{c}L^{c}G-OH, which ranked in the bottom 10% of the library, could not be detected up to ligand concentrations of 100 μM. These results suggest that the dominant epitope of 20D6.3 is -F^{c}L^c-. Consistent with this interpretation, 20D6.3 also binds AcY^{c}F^{c}L^{c}G-OH in solution with an IC_{50} on the order of 160 nM. Surprisingly, the fluorescence signal associated with this ligand ranked in the bottom 30% of the library, suggesting that the conformation of this ligand on the solid support may be different from that in solution (*24*). Nonetheless, the oligocarbamate library allowed us to rapidly determine the epitope of 20D6.3.

Because the oligocarbamate backbone (*25*) differs significantly from that of polypeptides one might expect differences in lipophilicity, hydrogen-bonding properties, stability, and conformational flexibility. Comparison of the water-octanol partition-

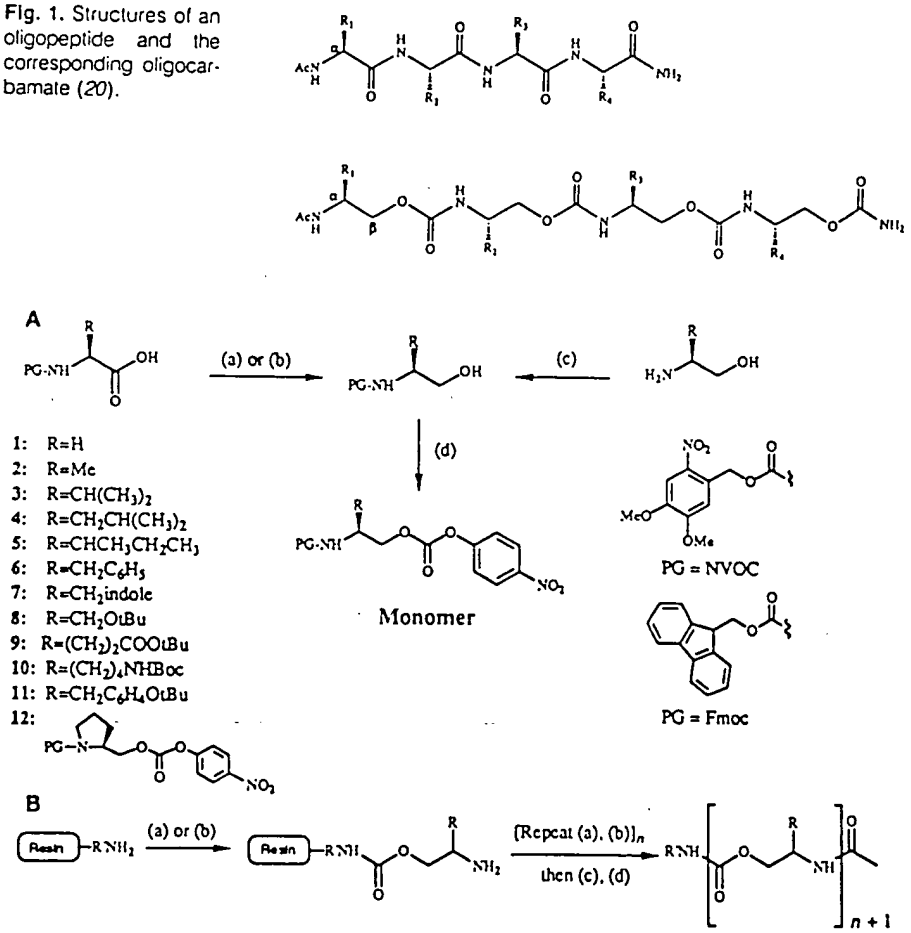

Fig. 1. Structures of an oligopeptide and the corresponding oligocarbamate (*20*).

Fig. 2. (A) Synthesis of activated *N*-protected *p*-nitrophenyl carbonate monomers: (a) BH_3, tetrahydrofuran; (b) DCC, CH_2Cl_2, *N*-hydroxysuccinimide, HOBt; then sodium borohydride, ethanol; c) NVOC-Cl or Fmoc-OSu, dioxane, $NaHCO_3$, H_2O; (d) *p*-nitrophenylchloroformate, CH_2Cl_2, pyridine. (B) Solid-phase synthesis of oligocarbamates: (a) monomer, HOBt, diisopropylethylamine, NMP; (b) piperidine, NMP; (c) acetic anhydride, NMP; and (d) trifluoroacetic acid, triethylsilane. R = H (Rink resin) (*16*) or amino acid (Wang resin) (*15*).

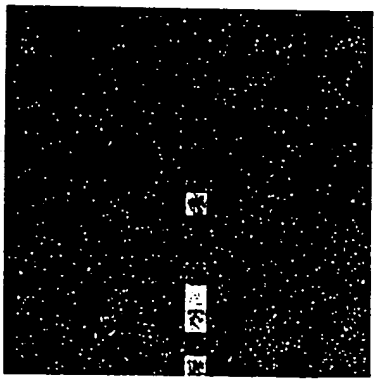

Fig. 3. Fluorescence intensities of oligocarbamate-antibody 20D6.3 complexes detected by using a goat α-mouse fluorescein-conjugated antibody. Each 800 μm by 800 μm square represents an individual member of the library.

ing coefficients (26) of the peptides AcYKFLG-OH (90) and AcYIFLG-OH (10) with the corresponding oligocarbamates AcY^{c}K^{c}F^{c}L^{c}G-OH (0.5) and AcY^{c}I^{c}F-^{c}L^{c}G-OH (0.4) revealed the latter to be significantly more hydrophobic. Moreover, oligocarbamates were significantly more resistant to proteolytic degradation than peptides. Treatment of the peptides AcYKFLG-OH and AcYIFLG-OH with trypsin or porcine pepsin, respectively, resulted in complete degradation within 20 min whereas the corresponding oligocarbamates showed no appreciable degradation after 150 min (27). These characteristics of oligocarbamates may be reflected in enhanced pharmacokinetic properties relative to oligopeptides. The structural and pharmacological properties of oligocarbamates and other polymers (such as substituted ureas and sulfones) may not only provide new tools for medicinal chemists buy may also provide new opportunities to construct two- and three-dimensional biopolymers with novel properties.

REFERENCES AND NOTES

1. R. B. Merrifield, *J. Am. Chem. Soc.* 85, 2149 (1963); *Science* 232, 341 (1986).
2. M. Hagihara, N. J. Anthony, T. J. Stout, J. Clardy, S. L. Schreiber, *J. Am. Chem. Soc.* 114, 6568 (1992); R. J. Simon *et al.*, *Proc. Natl. Acad. Sci. U.S.A.* 89, 9367 (1992).
3. A. M. Bray, N. J. Maeji, H. M. Geysen, *Tetrahedron Lett.* 31, 5811 (1990).
4. S. P. A. Fodor *et al.*, *Science* 251, 767 (1991).
5. R. A. Houghten *et al.*, *Nature* 354, 84 (1991).
6. K. S. Lam *et al.*, *ibid.*, p. 82 (1991).
7. J. Blake and L. Litzi-Davis, *Bioconjugate Chem.* 3, 510 (1992).
8. M. C. Needels *et al.*, *Proc. Natl. Acad. Sci. U.S.A.*, in press.
9. A. Eschenmoser and M. Dobler, *Helv. Chim. Acta.* 75, 218 (1992); A. B. Smith III *et al.*, *J. Am. Chem. Soc.* 114, 10672 (1992).
10. D. D. Weller, D. T. Daly, W. K. Olson, J. E. Summerton, *J. Org. Chem.* 56, 6000 (1991); J. M. Coull, D. V. Carlson, H. L. Weith, *Tetrahedron Lett.* 28, 745 (1987); W. S. Mungall and J. K. Kaiser, *J. Org. Chem.* 42, 703 (1977); B. R. Baker, P. M. Tanna, G. D. F. Jackson, *J. Pharm. Sci.* 54, 987 (1965).
11. J. C. Hanvey *et al.*, *Science* 258, 1481 (1992); E. Uhlmann and A. Peyman, *Chem. Rev.* 90, 543 (1990).
12. Reduction with this method yields optically pure amino alcohols: J. Nikawa and T. Shiba, *Chem. Lett.* 1979, 981 (1979). Single diastereomers were observed by ^{1}H nuclear magnetic resonance after carbamate couplings.
13. A. Patchornik, B. Amit, R. B. Woodward, *J. Am. Chem. Soc.* 92, 6333 (1970).
14. L. A. Carpino and G. Y. Han, *J. Org. Chem.* 37, 3404 (1972).
15. S.-S. Wang, *J. Am. Chem. Soc.* 95, 1328 (1973); G. Lu, S. Mojsov, J. P. Tam, R. B. Merrifield, *J. Org. Chem.* 46, 3433 (1981).
16. H. Rink, *Tetrahedron Lett.* 28, 3787 (1987).
17. D. S. King, C. G. Fields and G. B. Fields, *Int. J. Peptide Protein Res.* 36, 255 (1990).
18. E. Kaiser, R. L. Colescott, C. D. Bossinger, P. I. Cook, *Anal. Biochem.* 34, 595 (1970); V. K. Sarin, S. B. H. Kent, J. P. Tam, R. B. Merrifield, *ibid.* 117, 147 (1981).
19. Oligocarbamates were purified by preparative reversed-phase HPLC with a Whatman M-20 10/50 Partisil ODS-10 column at a flow rate of 8.0 ml/min and a linear gradient of 90%A/10%B to 0%A/100%B over 120 min; A, 0.1% trifluoroacetic acid (TFA)/H_2O; and B, 0.08% TFA/CH_3CN, 260 nm detection wavelength; followed by lyophilization.
20. Oligocarbamate sequences are designated by the names of the corresponding amino acids with a superscript c to indicate a carbamate bond. For example, the oligocarbamate where R_1 = *p*-hydroxybenzyl, R_2 = 1-aminobutyl, R_3 = benzyl, and R_4 = 2-methylpropyl is designated Ac-Y^{c}K^c-F^{c}L^c-NH$_2$, where Ac is acetyl. Abbreviations for the amino acid residues are: A, Ala; C, Cys; D, Asp; E, Glu; F, Phe; G, Gly; H, His; I, Ile; K, Lys; L, Leu; M, Met; N, Asn; P, Pro; Q, Gln; R, Arg; S, Ser; T, Thr; V, Val; W, Trp; and Y, Tyr.
21. Antibody was used directly from hybridoma cell culture supernatants: S. J. Pollack, P. Hsiun, P. G. Schultz, *J. Am. Chem. Soc.* 111, 5961 (1989).
22. Ligands of various concentrations in 50 mM tris-saline buffer, pH 7.4, were preincubated with antibody 20D6.3 (~1 μg/ml) for 1 hour at 37°C, transferred to Ac-Y^{c}K^{c}F^{c}L^{c}G-BSA–coated ELISA plates (5 μg/ml) for 2 hours at 37°C, and developed with goat-α-mouse alkaline phosphatase conjugate for 1 hour at 37°C followed by addition of *p*-nitrophenyl phosphate.
23. The NHS ester of the nitrophenylsulfenyl-protected hapten was coupled to keyhole limpet hemocyanin, and the resulting conjugate was deprotected by treatment with sodium dithionite to give a hapten to carrier density of 4.
24. The ligand AcY^{c}F^{c}L^c-OH (synthesized on glass via FMOC chemistry) also gave a low fluorescence signal when assayed against 20D6.3.
25. M. Oki and H. Nakanishi, *Bull. Chem. Soc. Jpn.* 44, 3148 (1971); S. van der Werf, R. Olijnsma, J. B. F. N. Engberts, *Tetrahedron Lett.* 689 (1967); C. M. Lee and W. D. Kumler, *J. Am. Chem. Soc.* 83, 4596 (1961).
26. Water:octanol partitioning coefficients were determined as described [J.-L. Fauchère and V. Pliska, *Eur. J. Med. Chem.* 18, 369 (1983)] by using 1-octanol and 10 mM phosphate buffer, pH 7.4 [final dimethylsulfoxide (DMSO) concentration 1%]. Concentration of ligands was determined spectrophotometrically by absorbance at 280 nm.
27. Trypsin (670 nM) was incubated at room temperature with either peptide substrate AcYKFLG-OH (630 μM) or carbamate ligand AcY^{c}K^{c}F^{c}L^{c}G-OH (420 μM) in tris-saline buffer, pH 7.4, containing 1% DMSO and 1% acetonitrile. Similarly, porcine pepsin (0.1 M formate buffer, pH 3.1, 1.1 μM) was incubated with peptide substrate AcYIFLG-OH (440 μM) or oligocarbamate AcY^{c}I^{c}F^{c}L^{c}G-OH (390 μM). Degradation of substrates was monitored by reversed-phase analytical HPLC.

28. This work was supported by the director, Office of Energy Research, Office of Biological & Environmental Research, General Life Sciences Division, of the U.S. Department of Energy under contract DE-AC03-76SF00098, by the Office of Naval Research (grant N00014-93-1-0380) and by a grant from the Lucille P. Markey Charitable Trust. E.J.M. was supported by the National Institutes of Health for a postdoctoral fellowship (grant 1 F32 GM14681). We also acknowledge Applied Biosystems for assistance in adapting oligocarbamate synthesis to the ABI automated synthesizer and J. Ellman and D. King for helpful discussions.

15 April 1993; accepted 23 July 1993

Discovery of Vapor Deposits in the Lunar Regolith

Lindsay P. Keller* and David S. McKay

Lunar soils contain micrometer-sized mineral grains surrounded by thin amorphous rims. Similar features have been produced by exposure of pristine grains to a simulated solar wind, leading to the widespread belief that the amorphous rims result from radiation damage. Electron microscopy studies show, however, that the amorphous rims are compositionally distinct from their hosts and consist largely of vapor-deposited material generated by micrometeorite impacts into the lunar regolith. Vapor deposits slow the lunar erosion rate by solar wind sputtering, influence the optical properties of the lunar regolith, and may account for the presence of sodium and potassium in the lunar atmosphere.

One of the expectations during the Apollo program was that the mineral grains in lunar soils would provide an opportunity to monitor the activity of the ancient sun and the properties of the solar wind as a function of time. However, it was soon realized that determination of the exposure history of individual grains was complicated by regolith processes, namely, meteoroid impact "gardening" on the lunar surface. Nevertheless, some workers tried to deduce the characteristics of the ancient solar wind from data acquired primarily from high-voltage transmission electron microscope (TEM) studies of the fine-grained fractions of lunar soils. It was discovered that many of the mineral grains in the submicrometer size range are surrounded by thin amorphous layers (*1*) that, it was demonstrated, could be produced by exposing mineral grains to a high flux of low-energy ions in the laboratory. This result suggested that the interaction of the solar wind with crystalline grains could produce the thin layer, where the crystallinity of the host grain was destroyed by implantation of solar wind ions (*2–4*). The concept that the amorphous rims are a result of radiation damage has been widely cited and is firmly ensconced in the literature. Our examination of the amorphous rims and their host grains shows, however, that most, if not all, of the amorphous rims formed primarily by the

Solar System Exploration Division, NASA Johnson Space Center, Houston, TX 77058.

*Present address: Lockheed, C23, 2400 NASA Road 1, Houston, TX 77258.